Progress in Organic Coatings 174 (2023) 107313

Contents lists available at ScienceDirect

Progress in Organic Coatings

journal homepage: www.elsevier.com/locate/porgcoat

Fabrication and performance of UV–curable Schiff base–containing antibacterial silicone modified materials

Xiongfa Yang [a,*], Yan Song [a], Yaohuang Jiang [b], Xiaoling Wang [c,*], Yina Yang [c], Jianhua Wang [d], Xiaojia Wang [a], Na He [a], Guoqiao Lai [a,*], Yanchun Yu [b,*]

[a] College of Material, Chemistry and Chemical Engineering, Key Laboratory of Organosilicon Chemistry and Material Technology of Ministry of Education, Key Laboratory of Silicone Materials Technology of Zhejiang Province, Hangzhou Normal University, Zhejiang 311121, China
[b] College of Life and Environmental Sciences, Hangzhou Normal University, Zhejiang 311121, China
[c] Sir Run Run Shaw Hospital, Affiliated Hospital of Medical School of Zhejiang University, Zhejiang 310020, China
[d] School of Resources and Chemical Engineering, Sanming University, Fujian, Sanming 365004, China

ARTICLE INFO

Keywords:
Antibacterial silicone modified materials
Schiff base
Transparent UV–curable materials
Hyperbranched silicone–containing polymers

ABSTRACT

There are numerous noxious bacteria, fungi and parasites in environment for human survival, so antibacterial materials are significant for medical devices, food packaging, and personal care. UV–curable silicone modified antibacterial materials were prepared from Schiff base–containing silicone modified hyperbranched thiol and castor oil based polyurethane acrylates (PUAs) by UV initiated thiol–ene click reaction. It exhibited that these UV–curable materials show fairly good antimicrobial activity of *Escherichia coli* (*E. coli*) and Neurospora crassa. A contact–kill antibacterial mechanism was proposed according to the antibacterial behavior of these UV–curable materials. These materials also exhibit a fairly high transparency over 92 % and pencil hardness can reach 4H. It need to be pointed out that the surface water contact angle of these materials is in the range of 84.1°–74.7°, which means these materials exhibit a certain degree of hydrophilicity, which can overcome the shortcoming of traditional polydimethylsiloxane(PDMS) to some content. These UV–curable materials show quite good mechanical performance because the tensile strength of them can reach 11.6 MPa. It denotes that the UV–curable Schiff base–containing antibacterial silicone modified materials may be a good candidate of antibacterial materials.

1. Introduction

Antibacterial materials are extensively used in fields such as medical devices, food packaging, and personal care due to numerous noxious bacteria, fungi and parasites in environment for human survival [1–4]. The most commonly used antibacterial reagents are antibiotics [5], however, the overuse of them is leading to worldwide antibiotics resistance crisis. Though nanoparticles of silver and metal oxides have drawn much attention for their good antibacterial performance [6], the applications of them will cause to toxicity on organisms [5,7]. Fabrication polymer composites with wonderful antibacterial capability by polymers and nanoparticles may be a promising solution, whereas there are some difficulties in making nanoparticles uniformly dispersed inside polymer matrixs [6]. To overcome these shortcomings, many covalently–antibacterial polymers were designed because of their merits of nonvolatile, stable chemical structure without losing their biological activity, difficulty to migrate, flexibility and easy processing [3,4,8,9].

Silicone polymers, especially polydimethylsiloxane (PDMS), are broadly used in biomedical field such as joint implants, catheters, kidney dialysis machines and breast prostheses because of their exceptional flexibility, biocompatibility, chemical and thermal stability, etc. [10–12]. Nonetheless, their hydrophobicity usually causes to serious

Abbreviations: E. coli, *Escherichia coli*; PDMS, polydimethylsiloxane; *S. aureus*, *Staphylococcus aureus*; SBSiHP, Schiff base–containing silicone modified hyperbranched thiol; PUAs, polyurethane acrylates; SBTSi, Schiff base–containing triethoxysilane; SHSi, (3–mercaptopropyl) trimethoxysilane; NPG, 2,2–dimethyl–1,3–propanediol; IPDI, isophorone diisocyanate; TMS, tetramethylsilane; FT–IR, Fourier–transform infrared spectroscopy; NMR, nuclear magnetic resonance; TGA, thermogravimetric analysis; PDA, Potato Dextrose Agar; LB, Luria–Bertani; SEC, size exclusion chromatography; DTG, derivative thermogravimetric analysis; DSC, differential scanning calorimetry; Tg, glass transition temperature.

* Corresponding authors.
E-mail addresses: yangxiongfa@hznu.edu.cn (X. Yang), 3203060@zju.edu.cn (X. Wang), laiguoqiao@aliyun.com (G. Lai), ycyu@hznu.edu.cn (Y. Yu).

https://doi.org/10.1016/j.porgcoat.2022.107313
Received 23 August 2022; Received in revised form 20 October 2022; Accepted 4 November 2022

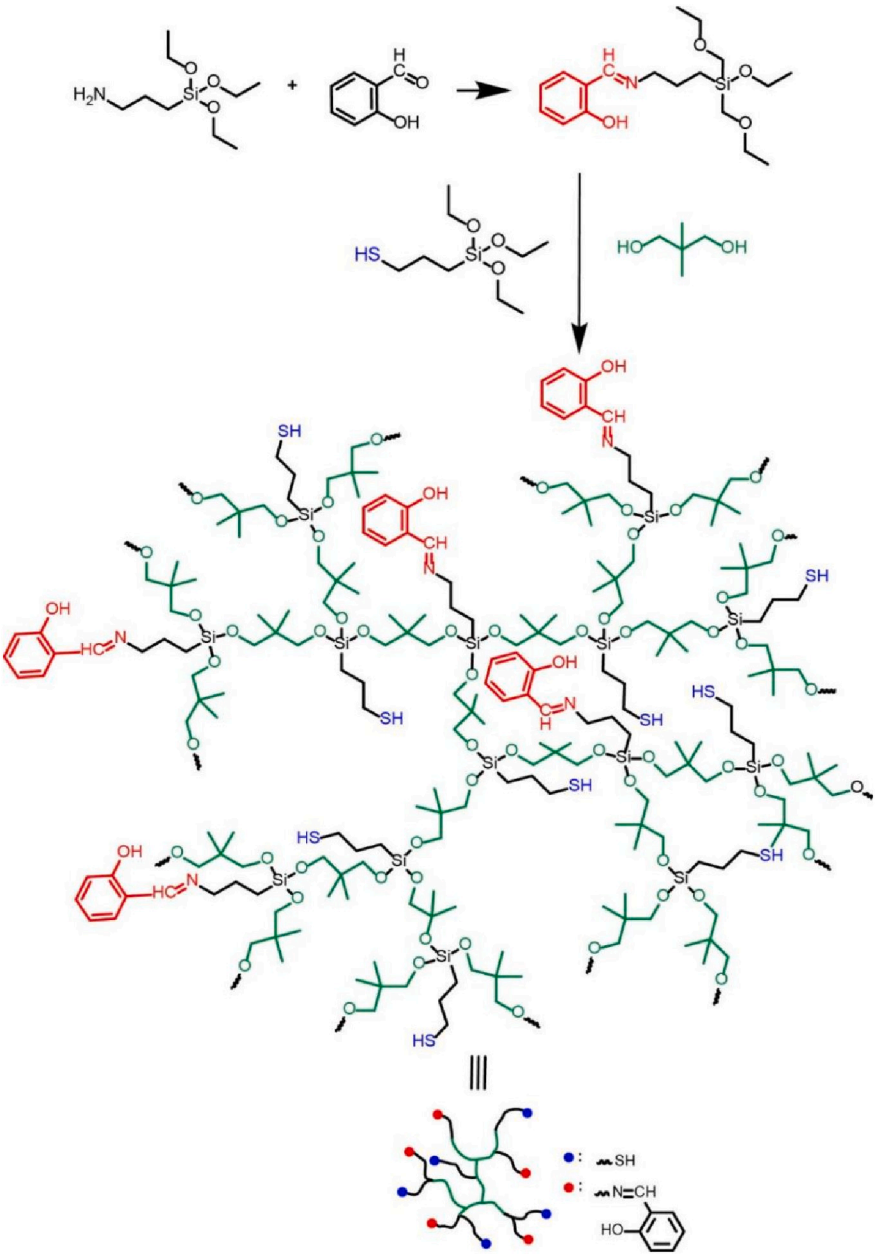

Scheme 1. Procedure for preparation of SBSiHPs.

health and economic implications attributed to the protein adsorption, bacterial contamination and biofilm formation [13,14]. To resolve these problems, antibacterial polymers were grafted onto the PDMS surface. Unfortunately, due to the good chemical stability, the surface of PDMS needs a sophisticated physical pretreatment such as oxygen plasma pretreatment to generate coupling sites [9,14]. As to the chemical modification strategies for PDMS surface, the first one is the hydrosilylation reaction between Si—H groups in the PDMS and C═C bonds in bioactive species [4,9,15], and the second one is the photo–induced 'grafting from' process of bioactive ingredients [3,9,16]. Nasreddine Kébir et al. [4] modified PDMS surface by grafting cationic polymers containing vinyl and quaternary ammonium groups, and the modified PDMS shows fairly good bactericidal effects against *E. coli* and *staphylococcus Epidermidis*. Lou et al. developed highly quaternary ammonium functionalized selfdisinfecting PDMS, which showed an efficient contact killing of *E. coli*, *Staphylococcus aureus* (*S. aureus*) and *Staphylococcus epidermidis* [3,11].They also introduced antibacterial polynorbornenes bearing quaternary phosphonium or pyridinium groups onto PDMS surfaces, which revealed an effective contact antibacterial effect against *E. coli* and *Staphylococcus epidermidis* [9]. Generally speaking, new strategies for developing silicone – containing polymer materials are highly desired.

Much attention have been paid to UV–curable materials in applications of coatings [17–19], personal care and package materials of food [20,21] due to the attractive advantages of UV–curing technology such as high efficiency, environmental protection and energy saving. As reported, Schiff base compounds have attracted more and more attention for their special biological activities such as antibacterial, antiviral, antitumor [18,19,22,23]. A Schiff base–containing coating with excellent surface bactericidal performance was fabricated from polyoxyethylene–bis–amine and tobramycin, which may be used broadly in bactericidal surfaces [24]. A cellulose–based Schiff base with good antibacterial activity was prepared from dialdehyde cellulose and L–lysine [25]. Inspired by these interesting works, it may be valuable to develop Schiff base–containing antibacterial UV–curable materials.

Furthermore, due to more and more strict environmental regulations

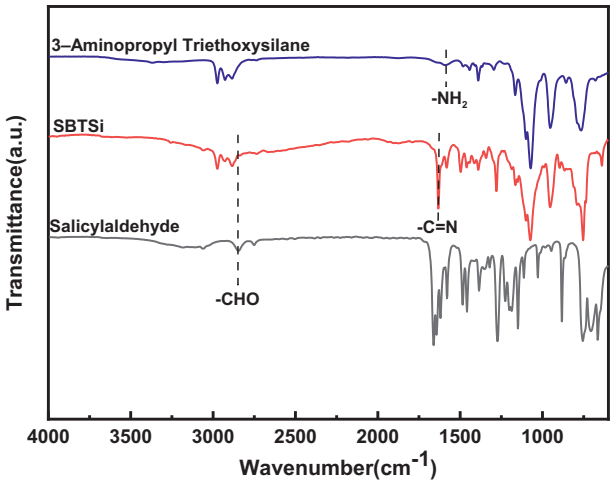

Fig. 1. FT–IR spectra of salicylaldehyde, 3–aminopropyl triethoxysilane and SBTSi.

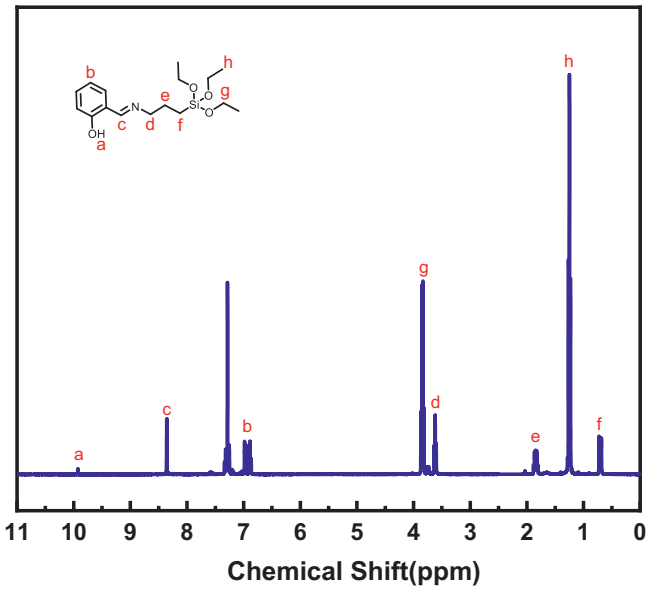

Fig. 2. ^{1}H NMR spectrum of SBTSi.

Table 1
Feed ratios of raw materials for preparation of SBSiHPs.

	Molar ratio of SBTSi to SHSi calculated by feed ratio	SBTSi/ g	SHSi/ g	NPG/ g	Molar ratio of SBTSi to SHSi calculated by ^{1}H NMR	Branch degree of SBSiHPs
SBSiHP-1	1:9	3.25	17.67	15.62	1/8.7	0.69
SBSiHP-2	3:7	9.76	13.74	15.62	3/6.9	0.68
SBSiHP-3	5:5	16.27	9.82	15.62	5/4.4	0.64
SBSiHP-4	7:3	22.78	5.89	15.62	7/3.0	0.61
SBSiHP-5	8:2	15.71	3.93	15.62	8/2.3	0.65

and world widely energy shortage crisis, as a kind of important renewable vegetable oils, castor oil has attracted growing attention to take the place of petroleum based materials in UV–curable materials [26,27]. In this paper, UV–curable silicone–modified antibacterial materials were prepared from Schiff base–containing silicone modified hyperbranched thiol (SBSiHP) and castor oil based polyurethane acrylates (PUAs) by UV initiated thiol–ene click reaction. These UV–curable materials with a fairly high transparency over 92 %, pencil hardness about 4H and tensile strength of 11.6 MPa show fairly good antimicrobial activity of *E. coli* and Neurospora crassa. A contact–kill antibacterial mechanism was proposed according to the antibacterial behavior of these UV–curable materials. Additionally, these materials can overcome the shortcoming of traditional PDMS to some content because they exhibit a certain degree of hydrophilicity for the surface water contact angle in the range of 84.1° to 74.7°.

2. Experimental section

2.1. Materials

2–Hydroxy–2–methyl–1–phenyl propanone (99.0 %, A. R.) was supplied by Hanghua Toka Ink Co., Ltd. (Hangzhou, China). Salicylaldehyde (A. R., 98 %) was bought from Aladdin reagent (Shanghai) Co., Ltd. (Shanghai, China). 3–Aminopropyltriethoxysilane (A. R., 99 %) was bought from Nanjing Capatue Chemical Co., Ltd. (Nanjing, China). *E. coli* (ATCC 25922), Neurospora crassa, ethanol (A. R., 99 %), (3–mercaptopropyl) trimethoxysilane (SHSi, A. R., 99 %) and 2,2–dimethyl–1,3–propanediol (NPG, A. R., 99 %) were from Shanghai Macklin Biochemical Co., Ltd. (Shanghai, China). Castor oil based PUAs were prepared according to reference [28] by the molar ratio of isophorone diisocyanate (IPDI) to castor oil of 2:1.

2.2. Preparation of SBSiHPs

All the operations were performed under a N_2 atmosphere. According to the Scheme 1, after 25.64 g (0.21 mol) salicylaldehyde was dissolved in 80 mL ethanol completely at 80 °C in a 250 mL three–necked flask, 46.50 g (0.21 mol) 3–aminopropyl triethoxysilane was added into by dropping funnel for about 2 h. The reaction solution was filtered and ethanol was removed with rotary evaporator after the reaction was conducted at 80 °C for another 5 h, then a yellow liquid of Schiff base–containing triethoxysilane (SBTSi) was produced.

The Fourier–transform infrared spectroscopy (FT–IR) analysis of salicylaldehyde, 3–aminopropyl triethoxysilane and SBTSi was conducted as shown in Fig. 1. It can be seen from the FT-IR spectra of salicylaldehyde and 3–aminopropyl triethoxysilane, the absorptions at about 2750 cm^{-1} and 2850 cm^{-1} were ascribed to be characteristic stretching vibration of —CHO in salicylaldehyde while the absorption at about 1591 cm^{-1} was ascribed to be characteristic stretching vibration of —NH_2 in 3–aminopropyl triethoxysilane. Obviously, there was absorption at about 1640 cm^{-1} ascribed to be characteristic C═N stretching band in SBTSi with the completely elimination of —CHO and —NH_2. The ^{1}H nuclear magnetic resonance (^{1}H NMR) spectra of SBTSi was also conducted and the assignment of the chemical shifts was shown in Fig. 2. The ^{1}H NMR of SBTSi with the integral ratios was shown in Fig. S1. Therefore, a conclusion can be draw that SBTSi was successfully prepared.

Later, according to the different feed molar ratios of SBTSi, SHSi and NPG shown in Table 1, several SBSiHPs were prepared according to reference [28,29]. To determine the chemical structure of SBSiHPs, ^{1}H NMR analysis with integral area was conducted as list in Fig. S2. Then, ^{1}H NMR, ^{13}C NMR, ^{29}Si NMR and size exclusion chromatography (SEC) analysis of SBSiHP–2 were exhibited in Figs. S3–6. The branch degree of SBSiHPs was calculated with the equation of DB = (D + T) / (D + T + L) according to the reference [30]. Where D, T, and L represent the fractions of the dendritic, terminal, and linear units, respectively, as shown

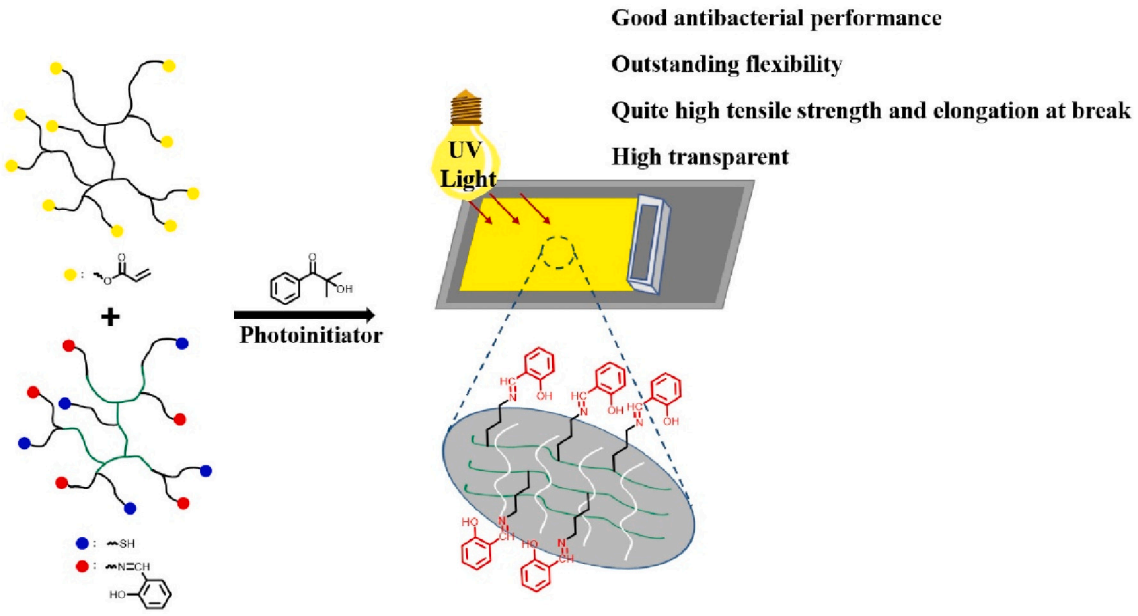

Scheme 2. Procedure for preparation UV–curable Schiff base–containing antibacterial silicone modified materials.

Table 2
Impact of UV curing time on the UV–curable materials.

Time/ s	The degree of curing content /%	Water absorption/ %	Pencil hardness
10	*48.8*	–	–
20	*57.1*	–	–
30	*69.7*	*18.7*	*6B*
40	*77.8*	*9.9*	*4B*
60	*83.7*	*8.6*	*2B*
80	*88.3*	*6.9*	*H*
90	96.3	0.71	*4H*
100	*96.7*	*0.60*	*4H*

Conditions: The SBSiHP is SBSiHP–2. The molar ratio of thiol groups to acrylate is 1:2.5 and the amount of 2–Hydroxy–2–methyl–1–phenyl propanone is 5 % of the total mass of SBSiHP–2 and castor oil based PUA.

by Fig. S7.

2.3. Preparation of UV–curable Schiff base–containing antibacterial silicone modified materials

The procedure for fabrication of UV–curable Schiff base–containing antibacterial silicone modified materials was exhibited by Scheme 2. A certain amount of SBSiHPs, castor oil based PUAs and 2–hydroxy–2–methyl–1–phenyl propanone were mixed homogeneously for about 5 min. To investigate the coating performance of UV–curable material, about 0.4 g mixtures were deposited on half of glass slides. After removal of bubbles completely for about 20 min by vacuum oven at room temperature, they were cured by UV (ZB1000, Changzhou Zibo Electron Technology Co., Ltd., Laser wavelength 365 nm, Radiation intensity 10.6 mW·cm^{-2}, the distance of the slides to the light is 20 cm) to produce UV–curable Schiff base–containing antibacterial silicone modified materials with thickness about 0.7 mm. Similarly, about 0.1 g of the mixtures were deposited on the surface of 10 mm diameter circle of medical nonwoven fabrics for antibacterial performance investigation.

2.4. Characterization

^{1}H NMR and ^{13}C NMR were analyzed by a Bruker AVANCE AV400 (400 MHz) spectrometer and a Bruker AVANCE AV600 (600 MHz) spectrometer in $CDCl_3$ without tetramethylsilane (TMS) as internal reference, respectively. FT–IR with an ATR was conducted on a Nicolet 700 spectrometer (Nicolet Co., Ltd., American). Transparency of the materials were measured on an UH5300 double–beam UV/Vis spectrophotometer (Hitachi Instrument Co., Ltd., Japan) in the range of 400–800 nm. Degree of curing contents were calculated as a percentage of the residual mass in the original mass of the cured coatings after the cured samples were washed with toluene by Soxhlet extration at 150 °C for 4 h. Adhesion property was analyzed by a BGD–502 paint film according to ISO 2409–2007 with cross cut test. The water absorption was analyzed according to "Determination of water absorption rate of insullac films" HGT 3856–2006. Surface water contact angle was measured according to "Measurement of water–contact angle of plastic films", GB/T 30693–2014 on a KRUSS DSA30 water contact angle meter (KRÜSS, Germany). Differential scanning calorimetry (DSC) of these coatings were conducted on a DSC Q100 apparatus (TA Instruments, New Castle, USA) under N_2 atmosphere. These samples were heated to 70 °C, held for 2 min to erase the thermal history, then cooled to −60 °C at a rate of 10 °C min^{-1}, and finally heated again to 70 °C at a heating rate of 10 °C min^{-1}. Thermogravimetric analysis (TGA) was measured using a TG 209C apparatus (NETZSCH–Gerätebau GmbH, Germany) under N_2 atmosphere from room temperature to 800 °C at a rate of 10 °C min^{-1}. Tensile test of the films (60 mm × 8 mm × 0.7 mm strips) scraped from the slides was carried out according to GB/T 528–2009/ISO 37:2005 on an UH6503D electronic tensile testing machine (Optimal Hung Measurement & Control Technology (Shanghai) Co. Ltd.) with load of 100 N at a loading rate of 60 mm/min. Neurospora crassa and *E. coli* were selected to investigate the antifungus and antibacterial performance, respectively. Potato Dextrose Agar (PDA) and Luria–Bertani (LB) were used as medium for the test of antifungus and antibacterial after high pressure damp heat sterilization at 121 °C for 25 min, respectively. The bacteria/fungal species were placed on the solid medium by twice–crossed method. The activated strains were added into 50 mL corresponding liquid medium and kept in the shaking bed for 24 h to produce bacterial suspension at 37/28 °C under 180 r/min. Subsequently, 5 μL corresponding bacterial suspensions were dropped on the coating surface. After the bacterial suspensions were dried, the coatings were sealed and kept in a shaking bed for 1–5 d at 37/28 °C with the control samples to observe the plaque size and morphology.

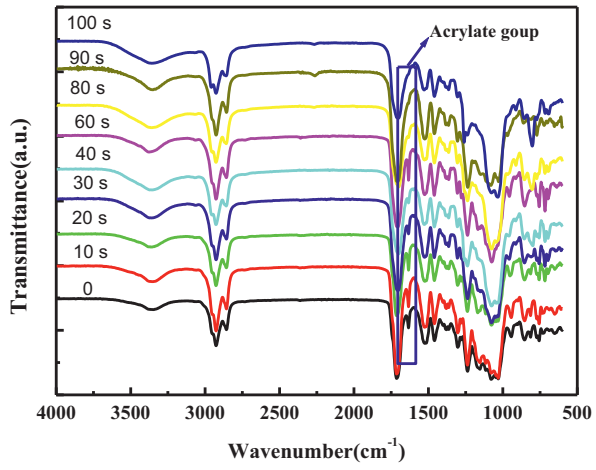

a The total spectra

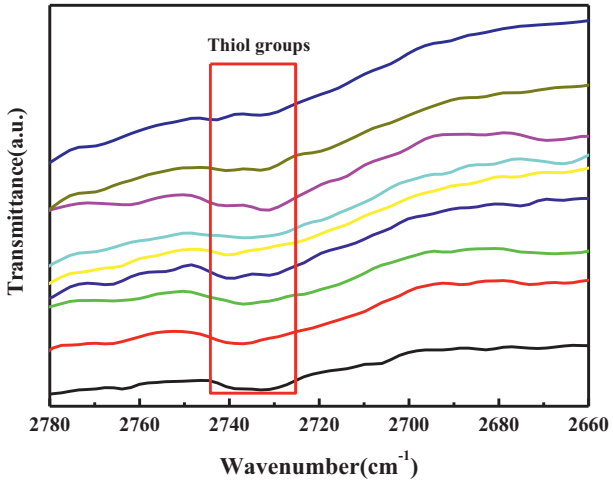

b The enlarged spectra for thiol groups

Fig. 3. FT–IR spectra of UV–curable materials produced by different UV curing time.
a The total spectra.
b The enlarged spectra for thiol groups.

Table 3
Effect of different SBSiHPs on the coating performance.

Different SBSiHPs	Molar ratio of SBTSi to SHSi	The degree of curing content/%	Water absorption/ %	The surface water contact angle/°	Pencil hardness
SBSiHP-1	1:9	98.3	0.47	84.1	4H
SBSiHP-2	3:7	96.3	0.71	82.8	4H
SBSiHP-3	5:5	92.5	0.98	81.8	2H
SBSiHP-4	7:3	91.3	1.21	79.9	2H
SBSiHP-5	8:2	90.1	2.33	74.7	2B

Conditions: The molar ratio of thiol groups to acrylate is 1:2.5. The other conditions are the same as Table 2.

Table 4
Effect of different molar ratio of thiol group to acrylate group on the coating performance of UV–curable materials.

The molar ratio of thiol group to acrylate group	The degree of curing content /%	Water absorption/ %	The surface water contact angle/°	Pencil hardness	Cross–linking density/(g/ mL)
1:0.6	74.1	1.8	78.4	6B	0.73
1:0.8	82.3	1.0	78.8	6B	0.77
1:1	89.9	0.87	78.1	6B	0.80
1:1.2	90.1	0.75	79.4	4B	0.81
1:1.5	90.3	0.71	79.1	3B	0.84
1:2.5	91.3	1.21	79.9	2H	1.47
1:3.0	93.4	1.21	84.7	4H	1.59

Conditions: The SBSiHP is SBSiHP–4. The other conditions are the same as Table 3.

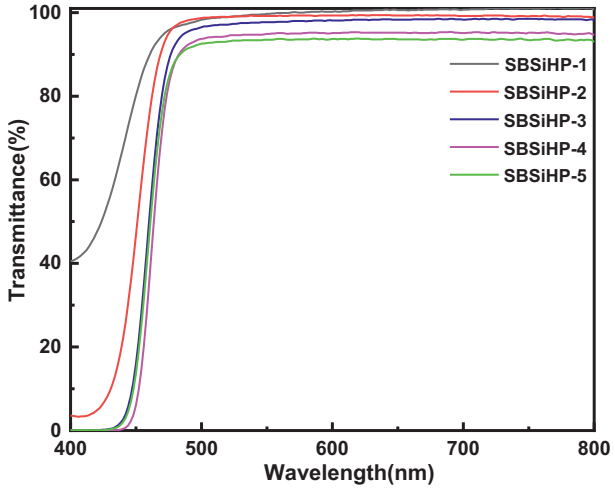

Fig. 4. Transparency of the UV–curable materials prepared with different SBSiHPs.

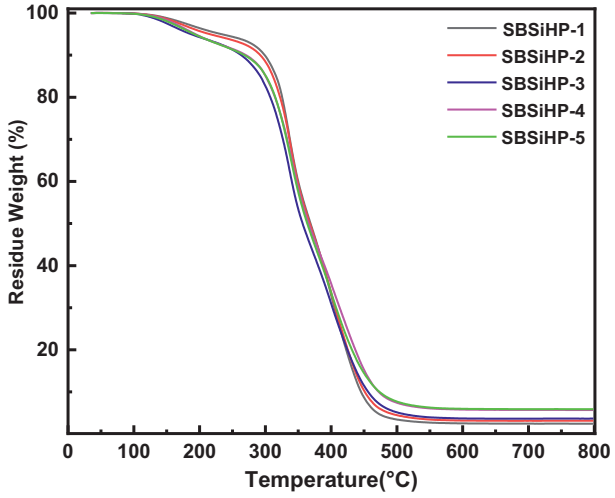

Fig. 5. TGA curves of the UV–curable materials prepared with different SBSiHPs.

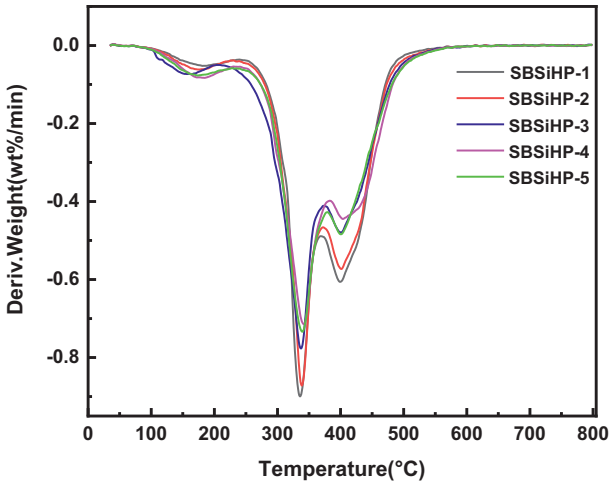

Fig. 6. DTG curves of the UV–curable materials prepared with different SBSiHPs.

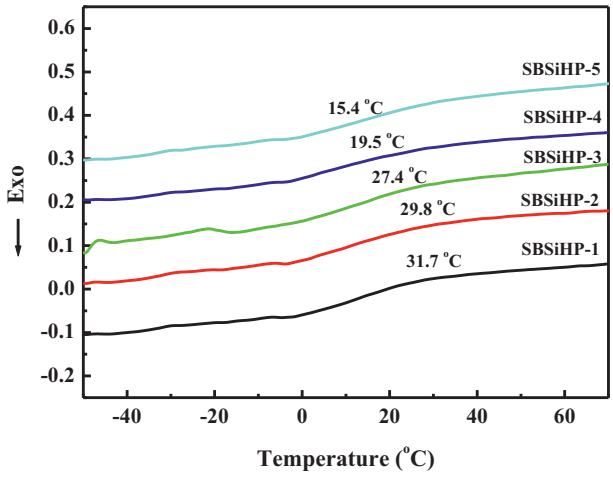

Fig. 7. DSC curves of the UV–curable materials prepared with different SBSiHPs.

3. Results and discussion

3.1. Fabrication of UV–curable Schiff base–containing antibacterial silicone modified materials

3.1.1. Impact of different UV curing time

The impact of different UV curing time on the properties of UV–curable Schiff base–containing antibacterial silicone modified materials was exhibited in Table 2. When the UV curing time is 10–20 s, a quite sticky soft coating with the degree of curing content in the range of 48.8 %–57.1 % can be produced. If the UV curing time propagated from 30 s to 90 s, the degree of curing content and pencil hardness increased from 69.7 % to 96.3 % and 6 B to 4H, respectively. On the contrary, water absorption decreased from 18.7 % to 5.7 % attributed to the increment of the cross–linking density of the UV–curable materials [28,29]. A further prolongation of UV curing time will have little effect on the properties of the materials.

The optimum UV curing time was determined by FT–IR analysis of UV–curable materials prepared by different UV curing time presented in Fig. 3. The absorptions at about 2750–2720 cm^{-1} and 1633 cm^{-1} ascribed to be characteristic peaks of thiol groups in SBSiHP–2 and acrylic groups in castor oil based PUA respectively, which were faded when the UV curing time prolonged to 90 s. In brief, the FT–IR analysis

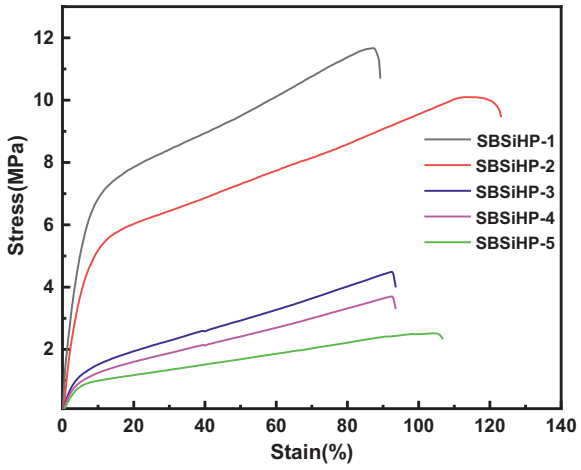

a UV–curable materials prepared with different SBSiHPs

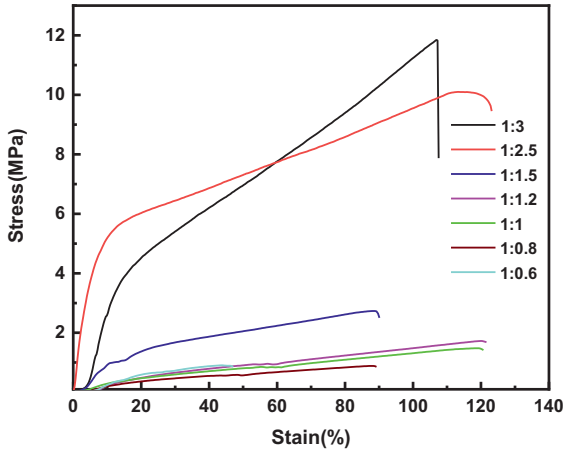

b UV–curable materials prepared with different molar ratio of thiol group to acrylate group

Fig. 8. Tensile–strain curves of the UV–curable materials.
a UV–curable materials prepared with different SBSiHPs.
b UV–curable materials prepared with different molar ratio of thiol group to acrylate group.

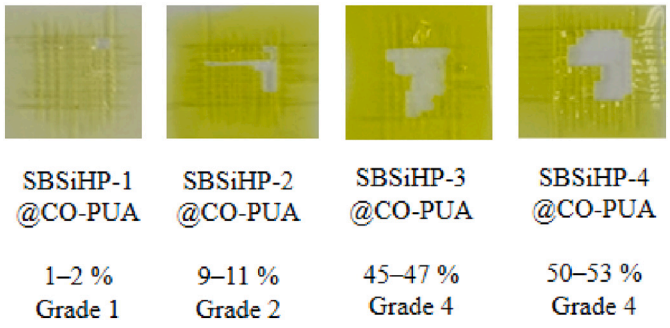

Fig. 9. Adhesive property to the glass slide of the UV–curable materials prepared with different SBSiHPs.

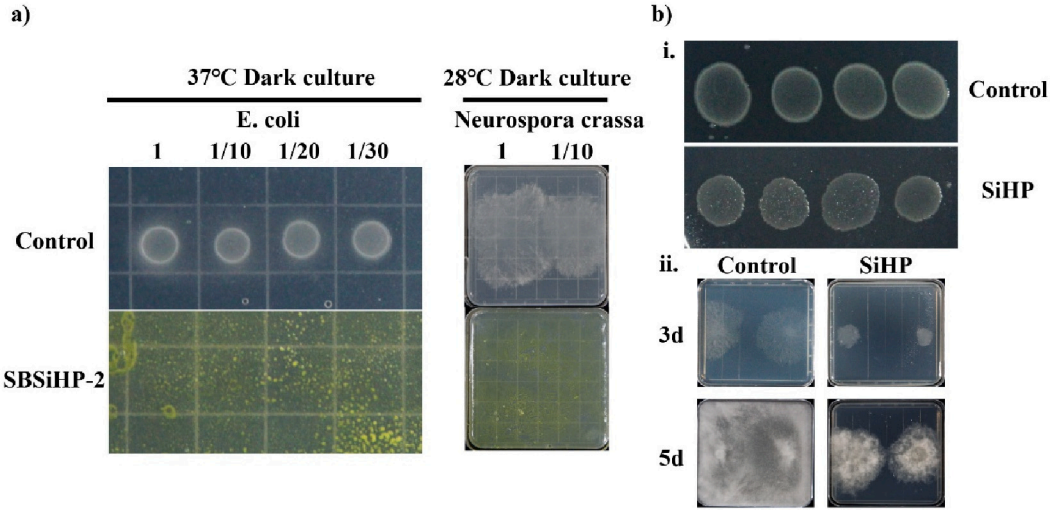

Fig. 10. Antibacterial performance of SBSiHPs.

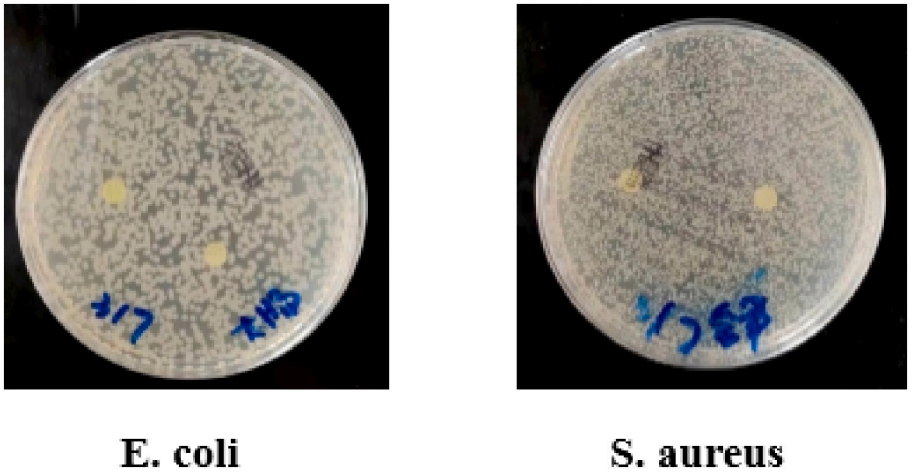

Fig. 11. Antibacterial performance of *E. coli* and *S. aureus* using inhibition zone method.

can be an important evidence that the optimum UV curing time is 90 s.

3.1.2. Effect of different SBSiHPs

Different SBSiHPs were synthesized according to the feed ratios list in Table 1 and the effect of them on the coating performance was summarized in Table 3. Apparently, when the molar ratio of SBTSi to SHSi increased from 1:9 to 8:2, the degree of curing content and pencil hardness of the materials decreased from 98.3 % to 90.1 % and 4H to 2 B, respectively. It need to be pointed out that the surface water contact angle of these materials decreased from 84.1° to 74.7°, which means these materials exhibit a certain degree of hydrophilicity. As reported, the hydrophobicity of PDMS limits its application for the serious health and economic implications [13,14]. From this point, the UV–curable Schiff base–containing antibacterial silicone modified materials can overcome this shortcoming to some content.

3.1.3. Effect of different molar ratio of thiol group to acrylate group

As reported, the molar ratio of thiol group to acrylate group has a key impact on the performance of cross–linking density of the UV–curable materials, which will have an important impact on the performance of the materials [28,29]. Table 4 collected the effect of different molar ratio of thiol group to acrylate group on the coating performance of these materials. A conclusion can be drawn that with the increment of the molar ratio of thiol group to acrylate group from 1:0.6 to 1:1.5, the degree of curing content, water absorption and pencil hardness increased incessantly from 74.1 % to 90.3 %, 1.8 % to 0.71 and 6 B to 3 B, respectively, which attributed to the increment of the cross–linking density from 0.73 g/mL to 0.84 g/mL [28,29]. The molar ratio of thiol group to acrylate group has almost no impact on the surface water contact angle of these materials(78.4–79.4°) and the hydrophilicity of these UV–curable materials will benefit the antibacterial properties of the UV–curable Schiff base–containing antibacterial silicone modified materials [13,14].

3.2. Performance of UV–curable Schiff base–containing antibacterial silicone modified materials

3.2.1. Transparency

The transparency of these materials was also studied as shown in Fig. 4. Generally speaking, the transparency of these materials decreased with the increment of the molar ratio of SBTSi to SHSi, which implies that the increment of the content of SBTSi will sacrifice the compatibility of SBSiHPs with castor oil based PUA. Nevertheless, these materials exhibit a fairly high transparency over 92 %.

3.2.2. Thermal properties

Thermal stability of these materials was measured by TGA. It can be seen from TGA curves shown in Fig. 5 that the initial thermal

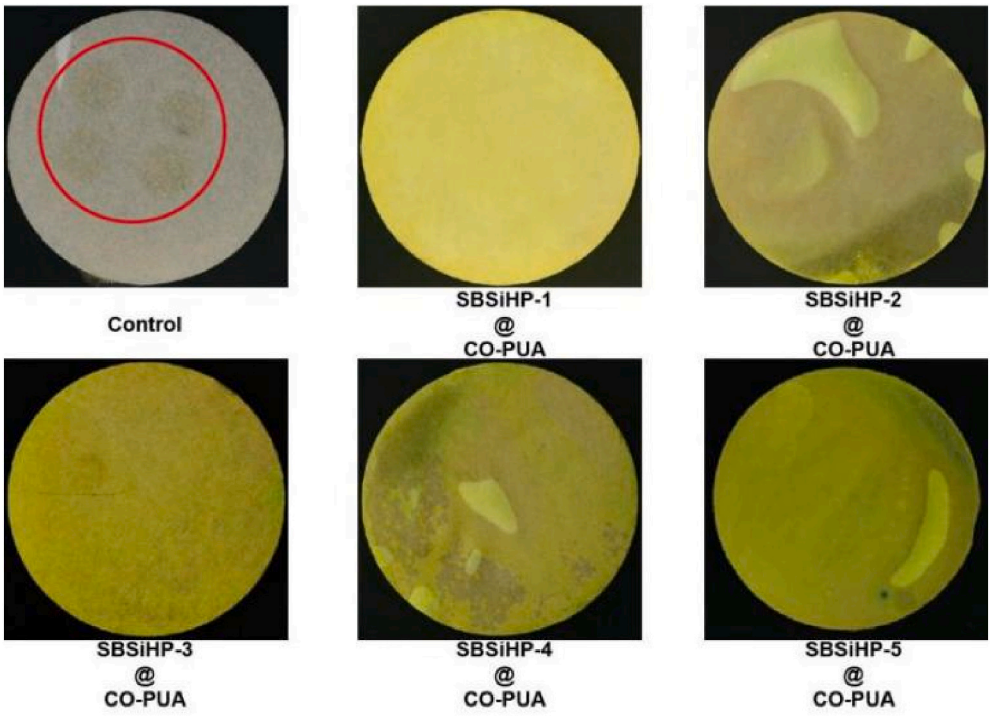

Fig. 12. Antibacterial performance of *E. coli* deposited on the circular surface of the UV–curable materials.

decomposition (T_{d5}) is in the range of 219–251 °C and the char yield of them increased with the increment of the molar ratio of SBTSi to SHSi. As reported, the conventional PUs will undergo severe pyrolysis when the temperature exceeds 200 °C [31–33]. Evidently, the UV–curable materials show obvious superior thermal stability than that of conventional PUs. The good thermal stability of these UV–curable materials is contributed by the silicone–containing segments and rigid benzene ring in SBSiHPs [33,34].

As can be seen from derivative thermogravimetric analysis (DTG) curves shown in Fig. 6, there are three thermal decomposition stages. The first thermal decomposition stage in the range of 104–253 °C may be ascribed to the thermal decomposition of PUA segments and UV initiator 2–Hydroxy–2–methyl–1–phenyl propanone. The second thermal decomposition stage in the range of 258–383 °C may be ascribed to the thermal decomposition of the Schiff base segments because the decomposition rate reduced with the increment of the molar ratio of SBTSi to SHSi. The third thermal decomposition stage in the range of 385–490 °C may be ascribed to the thermal decomposition of silicone–containing segments and rigid benzene ring introduced by SBTSi.

The results of DSC curves shown in Fig. 7 indicate that the Tg values of these UV–curable materials decrease from 31.7 °C to 15.4 °C with the molar ratio of SBTSi to SHSi increased from 1:9 to 8:2. It is due to the increment of the cross–linking density of these UV–curable materials attributed by a higher SHSi content in SBSiHPs, due to the motion of the molecule is hindered, which leads to a high Tg [29,33,35,36].

3.2.3. Mechanical properties

High tensile strength UV–curable silicone modified materials are highly desired [28,29]. As shown by Fig. 8a, the tensile strength of these materials decreased from 11.6 MPa to 2.5 MPa when the molar ratio of SBTSi to SHSi increased from 1:9 to 8:2. The elongation at break of these materials is in the range of 87–120 %, which implies these materials show fairly good flexibility. When the molar ratio of SBTSi to SHSi is 3:7, the elongation at break is the highest (about 120 %).

Additionally, the effect of molar ratio of thiol group to acrylate group on the tensile strength of these UV–curable materials prepared with SBSiHP–4 also investigated as shown in Fig. 8b. The tensile strength increased continuously from 0.9 MPa to 11.85 MPa with the decrement of the molar ratio of thiol group to acrylate group from 1:0.6 to 1:3.0, which also attributed to the increment of the cross–linking density of these materials.

The tensile strength of unreinforced pure silicone materials is not higher than 0.4 MPa [37–39] and that of commercial silicone elastomers is still no more than 2.4 MPa [40,41]. Evidently, the UV–curable materials obtained show superior tensile strength than the pure silicone materials and commercial silicone elastomer reported. Our group prepared UV cured transparent silicone modified PUAs with fairly high tensile strength of 3.40 MPa from hyperbranched silicon–containing polymers and petroleum based PUAs [29] and castor oil based high transparent UV cured silicone modified PUAs by silicon resins with tensile strength as high as 10.20 MPa [28]. Compared with these UV–curable materials, the UV–curable Schiff base–containing antibacterial silicone modified materials also exhibit fairly good tensile strength.

3.2.4. Adhesive property

The good adhesive property is highly desired for coatings, optical device packaging materials and antibacterial materials. It can be seen from Fig. 9 that the adhesive property turn worst from grade 1 to grade 4 with the increasing molar ratio of SBTSi to SHSi from 1:9 to 7:3. Earnestly, when the molar ratio of SBTSi to SHSi is 8:2, the adhesive property of the UV–curable material is too bad to be measured.

3.2.5. The antibacterial property

Antibacterial materials are highly desired and the antibacterial performance of SBSiHPs was examined firstly. As shown in Fig. 10, the samples prepared with different concentration of SBSiHP–2 have excellent surface antibacterial performance to both *E. coli* and Neurospora crassa.

Subsequently, the surface antibacterial performance of UV–curable materials prepared with different molar ratio of thiol group to acrylate group was examined. The antimicrobial performance of these UV–curable materials were assessed by observing the growth and development of *E. coli* and *S. aureus* using inhibition zone method of

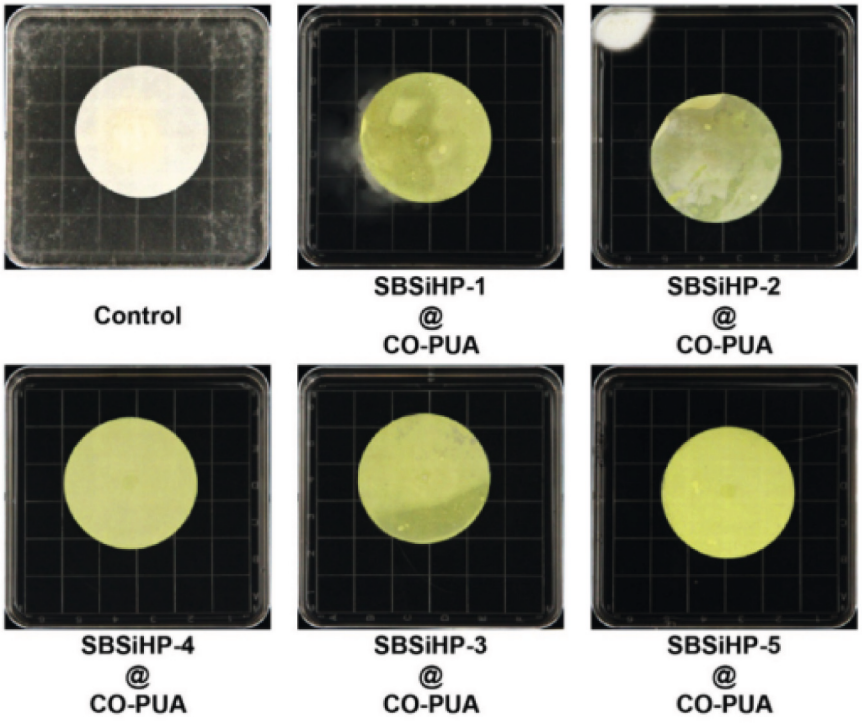

Fig. 13. Antibacterial performance of Neurospora crassa deposited on the circular surface of the UV–curable materials.

Kirby–Bauer test (Fig. 11), however, it can be obviously seen that there were almost no visible bacteriostatic zone around the samples on the culture dishes. Simultaneously, the antimicrobial performance of them were also assessed by observing the growth and development of *E. coli* and Neurospora crassa deposited on the circular surface of the UV–curable materials prepared from SBSiHP–2 choosing medical non–woven fabric as control sample(Figs. 12 and 13). As exhibited by Figs. 12 and 13, both the *E. coli* and Neurospora crassa were growing normally in control sample. In sharp contrast, these UV–curable materials showed a fairly good antimicrobial effect on the growth of *E. coli* and Neurospora crassa. In addition, the antimicrobial effect gradually turned better with the increasing molar ratio of SBTSi to SHSi from 1:9 to 7:3 attributed to the increment of Shiff base groups in the UV–curable materials. According to the result of inhibition zone test, it can be concluded that the

UV–curable materials can be considered as a non–dissolution contact type antibacterial type [42]. Therefore, combination the antibacterial behavior observed in the growth and development of *E. coli* and Neurospora crassa deposited on the circular surface of the UV–curable materials, it can be proposed that the antibacterial behavior of these UV–curable materials follow a contact–kill antibacterial mechanism [42–44].

4. Conclusions

UV–curable silicone modified antibacterial materials were prepared from SBSiHP and castor oil based PUAs by UV initiated thiol–ene click reaction. It exhibited that these UV–curable materials show fairly good antimicrobial activity of *E. coli* and Neurospora crassa. The antimicrobial activity increased with the increasing of molar ratio of SBTSi to SHSi. A contact–kill antibacterial mechanism was proposed according to the antibacterial behavior of these UV–curable materials. These materials exhibit a fairly high transparency over 92 % and pencil hardness can reach 4H. These UV–curable materials show quite good mechanical performance because the tensile strength of them can reach 11.6 MPa. These UV–curable materials may be a good candidate of UV–curable antibacterial materials and the practical applications of them in inhibition of harmful bacteria and fungi in home and hospital environment will be investigated.

Declaration of competing interest

The authors declare that we have no known competing financial interests or personal relationships that could have appeared to influence the work reported in this paper

Data availability

No data was used for the research described in the article.

Acknowledgment

The authors are grateful for financial support from Hanghua Toka Ink Co., Ltd. (2021HSN257).

Appendix A. Supplementary data

Fig. S1: ^{1}H NMR of SBTSi with the integral ratios. Fig. S2: ^{1}H NMR of SBSiHPs. Figs. S3–5:^{1}H NMR, ^{13}C NMR and ^{29}Si NMR spectra of SBSiHP–2. Fig. S6: SEC curve of SBSiHP–2. Fig. S7: The dendritic, terminal and linear units of SBSiHPs. Supplementary data to this article can be found online at https://doi.org/10.1016/j.porgcoat.2022.107313.

References

[1] X.M. Liang, X. Chen, J.L. Zhu, L.X. Liu, W. Wang, X. Wang, C.S. Qu, A simple method to prepare superhydrophobic and regenerable antibacterial films, Mater. Res. Express 7 (2020), 055307.
[2] H. Gu, S.W. Lee, J. Carnicelli, T. Zhang, D.C. Ren, Magnetically driven active topography for long–term biofilm control, Nat. Commun. 11 (1) (2020) 1–11.
[3] Y.Z. Lou, D. Schapman, D. Mercier, S. Alexandre, F. Burel, P. Thebault, N. Kébir, Self–disinfecting PDMS surfaces with high quaternary ammonium functionality by direct surface photoinitiated polymerization of vinylbenzyl dimethylbutylammonium chloride, Eur. Polym. J. 152 (2021), 110473.
[4] N. Kébir, I. Kriegel, M. Estève, V. Semetey, Preparation of bactericidal cationic PDMS surfaces using a facile and efficient approach, Appl. Sur. Sci. 360 (2016) 866–874.
[5] W. Peng, H. Yin, P.M. Liu, J.M. Peng, J. Sun, X. Zhang, Y.H. Gu, X.H. Dong, Z. Z. Ma, J. Shen, P.S. Liu, Covalently construction of poly(hexamethylene biguanide) as high–efficiency antibacterial coating for silicone rubber, Chem. Eng. J. 412 (2021), 128707.
[6] S. Kheiri, M.G.A. Mohamed, M. Amereh, D. Roberts, K. Kim, Antibacterial efficiency assessment of polymer–nanoparticle composites using a high–throughput microfluidic platform, Mat. Sci. Eng. C 111 (2020), 110754.
[7] S.S. Wang, Y.Y. Wang, Y. Peng, X.M. Yang, Exploring the antibacteria performance of multicolor Ag, Au, and Cu nanoclusters, ACS Appl. Mater. Inter. 11 (8) (2019) 8461–8469.
[8] J. Velazco-De-La-Garza, L. Avérous, E. Pollet, A. Zugasti-Cruz, C.A. Sierra-Rivera, E. Oyervides-Muñoz, G.de J. Sosa-Santillán, N.V. Pérez-Aguilar, Biological properties of novel polysuccinimide derivatives synthesized via quaternary ammonium grafting, Eur. Polym. J. 131 (2020) 109705.
[9] Y.Z. Lou, D. Schapman, D. Mercier, N.C. Süer, T. Eren, P. Thebault, N. Kébir, Preparation of bactericidal PDMS surfaces by benzophenone photo–initiated grafting of polynorbornenes functionalized with quaternary phosphonium or pyridinium groups, Eur. Polym. J. 157 (2021), 110669.
[10] M. Bračič, O. Šauperl, S. Strnad, I. Kosalec, O. Plohl, L.F. Zemljič, Surface modification of silicone with colloidal polysaccharides formulations for the development of antimicrobial urethral catheters, Appl. Surf. Sci. 463 (1) (2019) 889–899.
[11] Y.Z. Lou, D. Schapman, D. Mercier, S. Alexandre, F. Burel, P. Thebault, N. Kébir, Preparation of bactericidal surfaces with high quaternary ammonium through photo–initiated polymerization of N–[2–(acryloyloxy)ethyl]–N, N–dimethyl–N–butylammonium iodide from native and thiolated PDMS surfaces, React. Funct. Polym. 165 (2021), 104941.
[12] N.N. Ashton, G. Allyn, S.T. Porter, T.J. Haussener, P.R. Sebahar, R.E. Looper, D. L. Williams, In vitro testing of a first–in–class tri-alkylnorspermidine–biaryl antibiotic in an anti–biofilm silicone coating, Acta Biomater. 93 (2019) 25–35.
[13] Q. Gao, M. Yu, Y.J. Su, M.H. Xie, X. Zhao, P. Li, P.X. Ma, Rationally designed dual functional block copolymers for bottlebrush–like coatings: in vitro and in vivo antimicrobial, antibiofilm, and antifouling properties, Acta Biomater. 51 (2017) 112–124.
[14] C. Donzel, M. Geissler, A. Bernard, H. Wolf, B. Michel, J. Hilborn, E. Delamarche, Hydrophilic poly (dimethylsiloxane) stamps for microcontact printing, Adv. Mater. 13 (15) (2001) 1164–1167.
[15] W. Mussard, N. Kebir, I. Kriegel, M. Estève, V. Semetey, Facile and efficient control of bioadhesion on poly (dimethylsiloxane) by using a biomimetic approach, Angew. Chem. Int. Ed. 123 (46) (2011) 11063–11066.
[16] B.L. Leigh, E. Cheng, L. Xu, A. Derk, M.R. Hansen, C.A. Guymon, Antifouling photograftable zwitterionic coatings on PDMS substrates, Langmuir 35 (5) (2018) 1100–1110.
[17] Y. Chen, Q. Chen, Z.D. Wang, Z.Q. Yan, Q. Zhang, Q.X. Han, Bactericidal silicone with one quaternary ammonium salt and two N–halamine sites in the repeating unit for improved biocidability on magnetic submicrospheres, J. Mater. Sci. 57 (2022) 2100–2114.
[18] S.S. Yang, X.J. Wang, Z.Q. Hu, D.C. Guo, AIE and ESIPT schiff base ligands and corresponding Eu(III) complexes: multiple-color and fluorescence properties, Colloid Surf. A Phys. Eng. Asp. 615 (2021), 126293.
[19] X.C. Wang, G. Ding, Y.K. Duan, Y.J. Zhu, G.S. Zhu, M. Wang, X.J. Li, Y.F. Zhang, X. Z. Qin, C.H. Hung, A novel triphenylamine–based bis–schiff bases fluorophores with AIE activity as the hydrazine fluorescence turn-off probes and cell imaging in live cells, Talanta 217 (2020), 121029.
[20] X.Z. Ren, W.K. Liu, Q.C. Yao, S.Q. Wang, W.J. Liu, H. Gu, D.P. Wang, J.L. Fan, X. J. Peng, A UV–LED excited photoinitiator with low toxicity and low migration for photocurable inks, Dyes Pigments 200 (2022), 110133.
[21] J.Y. Zhou, X. Allonas, A. Ibrahim, X.X. Liu, Progress in the development of polymeric and multifunctional photoinitiators, Prog. Polym. Sci. 99 (2019), 101165.
[22] L.F. Xu, Q.Y. Meng, Z.Q. Zhang, S.L. Zhong, Y. Gao, X.J. Cui, Chitosan–salicylide schiff base with aggregation–induced emission property and its multiple applications, Int. J. Biol. Macromol. 209 (2022) 1124–1132.
[23] Y.M. Ahmed, G.G. Mohamed, Synthesis, spectral characterization, antimicrobial evaluation and molecular docking studies on new metal complexes of novel Schiff base derived from 4,6–dihydroxy–1,3–phenylenediethanone, J. Mol. Struct. 1256 (2022), 132496.
[24] N. Cao, R.J. Jiang, L.W. Hao, L.M. Tian, R. Mo, Y. Fan, J. Zhao, L.Q. Ren, Anti–adhesive and bactericidal polymeric coating based on Schiff–base reaction, Mater. Lett. 250 (2019) 182–185.
[25] L.M. Zhang, P.C. Yan, Y. Li, X.H. He, Y.J. Dai, Z.L. Tan, Preparation and antibacterial activity of a cellulose–based schiff base derived from dialdehyde cellulose and L–lysine, Ind. Crop. Prod. 145 (2020), 112126.
[26] B. Liang, J. Zhao, G. Li, Y. Huang, Z. Yang, T. Yuan, Facile synthesis and characterization of novel multi–functional bio–based acrylate prepolymers derived from tung oil and its application in UV–curable coatings, Ind. Crop. Prod. 138 (2019), 111585.
[27] B. Liang, R. Li, C. Zhang, Z. Yang, T. Yuan, Synthesis and characterization of a novel tri–functional bio–based methacrylate prepolymer from castor oil and its application in UV–curable coatings, Ind. Crop. Prod. 135 (2019) 170–178.
[28] F. Cheng, Y.X. Fan, N. He, Y. Song, J.B. Shen, Z.S. Gong, X.M. Tong, X.F. Yang, Castor oil based high transparent UV cured silicone modified polyurethane acrylate coatings with outstanding tensile strength and good chemical resistance, Prog. Org. Coat. 163 (2022), 106624.
[29] X.J. Jiao, J.L. Liu, J. Jin, F. Cheng, Y.X. Fan, L. Zhang, G.Q. Lai, X.L. Hua, X. F. Yang, UV cured transparent silicone materials with high tensile strength prepared from hyperbranched silicon–containing polymers and polyurethane–acrylates, ACS Omega 6 (4) (2021) 2890–2898.
[30] M.S. Chen, J.L. Wu, L.Z. Zhou, C.Y. Jin, C.L. Tu, B.S. Zhu, F.A. Wu, Q. Zhu, X. Y. Zhu, D.Y. Yan, Hyperbranched glycoconjugated polymer from natural small molecule kanamycin as a safe and efficient gene vector, Polym. Chem. 2 (2011) 2674–2682.

[31] A.K. Mishra, R. Narayan, T.M. Aminabhavi, S.K. Pradhan, K.V.S.N. Raju, Hyperbranched polyurethane (HBPU)–urea and HBPU–imide coatings: effect of chain extender and NCO/OH ratio on their properties, Prog. Org. Coat. 74 (1) (2012) 134–141.
[32] J. Pagacz, E. Hebdab, B. Janowskic, D. Sternikd, M. Janciab, K. Pielichowskib, Thermal decomposition studies on polyurethane elastomers reinforced with polyhedral silsesquioxanes by evolved gas analysis, Polym. Degrad. Stabil. 149 (2018) 129–142.
[33] J.L. Liu, X.J. Jiao, F. Cheng, Y.X. Fan, Y.F. Wu, X.F. Yang, Fabrication and performance of UV cured transparent silicone modified polyurethane–acrylate coatings with high hardness, good thermal stability and adhesion, Prog. Org. Coat. 144 (2020), 105673.
[34] S. Mapari, S. Mestry, S.T. Mhaske, Developments in pressure–sensitive adhesives: a review, Polym. Bull. 78 (2021) 4075–4108.
[35] A. Satdive, S. Mestry, P. Borse, et al., Phosphorus– and silicon–containing amino curing agent for epoxy resin, Iran. Polym. J. 29 (2020) 433–443.
[36] S. Arora, S. Mestry, D. Naik, et al., o–Phenylenediamine–derived phosphorus–based cyclic flame retardant for epoxy and polyurethane systems, Polym. Bull. 77 (2020) 3185–3205.
[37] Z. Sun, Q. Huang, Y.Z. Wang, L.Q. Zhang, Y.P. Wu, Structure and properties of silicone rubber/styrene–butadiene rubber blends with in situ interface coupling by thiol−ene click reaction, Ind. Eng. Chem. Res. 56 (6) (2017) 1471–1477.
[38] Q.G. Li, X.J. Huang, H. Liu, S.B. Shang, Z.Q. Song, J. Song, Preparation and properties of room temperature vulcanized silicone rubber based on rosin–grafted polydimethylsiloxane, RSC Adv. 8 (26) (2018) 14684–14693.
[39] Y.F. Wu, J.L. Liu, X.J. Jiao, F. Cheng, G.Q. Lai, X.F. Yang, UV cured transparent flexible silicone materials with high tensile strength, ACS Omega 5 (2020) 6199–6206.
[40] S.J. Park, K. Mondal, R.M. Treadway III, V. Kumar III, S.Y. Ma III, J.D. Holbery III, M.D. Dickey III, Silicones for stretchable and durable soft devices: beyond sylgard–184, ACS Appl. Matr. Inter. 10 (13) (2018) 11261–11268.
[41] J. Vaicekauskaite, P. Mazurek, S. Vudayagiri, A.L. Skov, Mapping the mechanical and electrical properties of commercial silicone elastomer formulations for stretchable transducers, J. Mater. Chem. C 8 (4) (2020) 1273–1279.
[42] T. Wei, Q. Yu, Chen Hong, Responsive and synergistic antibacterial coatings: fighting against bacteria in a smart and effective way, Adv. Healthcare Mater. (2019) 1801381.
[43] R. Bai, Q. Zhang, L.L. Li, P. Li, Y.-J. Wang, O. Simalou, Y.L. Zhang, G. Gao, A. Dong, N-Halamine–containing electrospun fibers kill bacteria via a contact/release Co–determined antibacterial pathway, ACS Appl. Mater. Interfaces 8 (2016) 31530–31540.
[44] J. Zhang, R.T. Zhou, H. Wang, X.Y. Jiang, H.Y. Wang, S.J. Yan, J.H. Yin, S.F. Luan, Bacterial activation of surface–tethered antimicrobial peptides for the facile construction of a surface with self–defense, Appl. Surf. Sci. 497 (2019), 143480.